Journal of Process Control 68 (2018) 23–33

Contents lists available at ScienceDirect

Journal of Process Control

journal homepage: www.elsevier.com/locate/jprocont

Growth rate maximization in fed-batch processes using high order sliding controllers and observers based on cell density measurement

Martín Jamilis*, Fabricio Garelli, Hernán De Battista

Grupo de Control Aplicado (GCA), Instituto LEICI, UNLP-CONICET, Facultad de Ingeniería, Universidad Nacional de La Plata, Argentina

ARTICLE INFO

Article history:
Received 29 April 2016
Received in revised form 7 March 2017
Accepted 9 April 2018

Keywords:
Fed-batch
Sliding mode
Extremum seeking
Gradient

ABSTRACT

A novel extremum seeking scheme is proposed for the optimization of the specific growth rate in fed-batch processes with substrate inhibited kinetics. The proposed controller is based on a high order sliding mode algorithm, which uses the gradient of the specific growth rate as switching coordinate. A gradient estimation is obtained through a high order sliding mode observer. Both the control and gradient estimation algorithms are finite-time stable. The stability of the controller is analysed using Lyapunov functions for both the unperturbed and perturbed cases and guidelines for the algorithm tuning are provided. The controller and observer algorithms are numerically assessed and simulation results are obtained for a set of different scenarios.

1. Introduction

In many biotechnological process applications it is important to optimize the reaction rates in order to obtain high productivities or favour metabolic states. For example, the maximization of the specific growth rate allows obtaining the largest amount of biomass for a given process duration. When the microorganism has non-monotonic kinetics (e.g. Haldane) there is a particular substrate concentration which maximizes the specific growth rate.

From the control viewpoint, on-line process optimization consists in regulating the specific growth rate at a given optimal value, or equivalently, in regulating the substrate at the optimal concentration. A wide variety of closed loop algorithms have been reported in the literature aimed at regulating growth rates or concentrations. For instance, closed loop versions of an exponential feeding law are given in [1–3], linearizing control is studied in [4] along with its stability for operating points at both sides of the optimum. Adaptive linearizing control is one of the most developed techniques [5–7], introducing the use of observers to estimate unmeasured variables or parameters. Also, growth rate regulation has been developed in [8,9] based on geometric invariance concepts. These approaches are able to deal with common issues such as parameter uncertainty and lack of on-line measurements. However, a previously known set-point or trajectory is required either for the regulation of the kinetic rates or concentrations.

Extremum-seeking control provides tools to accomplish real time optimization of the process. The basic concept of extremum seeking is to define a control action which allows searching an operating point where a given objective function is maximized (or minimized). A survey on the application of extremum seeking to bioreaction processes was done in [10] where two types of extremum seeking schemes are defined. First, the perturbation-based scheme where the process is treated as black-box and the objective function is not known but measured. The control technique consist in disturbing the input of the process with a dither signal, then an estimate of the gradient is obtained by filtering and modulating the measured output which is later used to define a control action. This type of scheme has been developed in depth in [11] and the application to a continuous tank reactor can be found in [12] for volumetric growth rate maximization. Similarly, in [13] the specific growth rate is maximized but the gradient estimation is obtained with a generalized super-twisting (GST) observer rather than by filtering and modulation. The second scheme is the model-based extremum seeking, where only the objective function structure is known but not the parameters values. These are estimated on-line and the location of the optimum is determined from the estimations resulting in an adaptive algorithm. Many examples can be found in the bibliography as in [7,14–16].

Both the perturbation-based and model-based techniques are equally valid. The first one requires minimum knowledge of the process but the process needs to be persistently disturbed and the final state is likely to oscillate around the optimal operating point. The model-based extremum seeking has the advantage that some degree of transient performance can be guaranteed. However, a

* Corresponding author.
E-mail address: martin.jamilis@ing.unlp.edu.ar (M. Jamilis).

https://doi.org/10.1016/j.jprocont.2018.04.003
0959-1524/

model structure needs to be assumed and included in the design, moreover, the dither signal is still used to ensure the excitation persistence necessary to estimate the parameters. Also, the resulting algorithms are generally more complex.

More recently, alternative approaches are being developed in the bioprocess control field in an attempt to bring together some of the advantages of the perturbation-based and model-based schemes. The goal is to design algorithms that do not rely vastly in the process models but giving certain guarantees on the transient response. Then, the objective function is unknown but its value can be measured or estimated from the process states. As it is necessary to disturb the plant to locate the optimum position, switched control algorithms like sliding mode control fit suitably for the task. The decision variable which produces the control switch can be in some cases an estimation of the error between the current and optimal substrate concentrations or the gradient of the objective function. In [17] a pseudo-super-twisting controller (PSTC) is proposed to maximize the gas production rate in an activated sludge process, where the substrate error is used as sliding coordinate. The sign of the error is estimated with a state machine analyzing the changes in the measured gas rate and the substrate. However. the magnitude of the error is estimated with a static function rather than with a closed loop algorithm. A similar approach is taken in [18] for the gradient estimation but using an output-feedback two-level controller instead of the PSTC. In [19] specific growth rate maximization is achieved with a first order sliding mode (FOSM) controller using an estimation of the gradient as sliding coordinate. The gradient estimation is obtained by the discrete estimator proposed in [20] using substrate concentration and gas production rate measurements. The growth rate is driven successfully to a neighborhood of the optimal value, however chattering issues are present, at least for gains large enough to reject the studied disturbances. These works have in common that both the control algorithms and decision variable estimations are run with a sample time large enough to let the output show some variation, which also introduces additional dynamics to the loop.

In this work, a new extremum seeking scheme is proposed to maximize the specific growth rate in fed-batch processes. The scheme is based on a high order sliding mode (HOSM) controller where the sliding coordinate is an estimation of the specific growth rate gradient with respect to the substrate. The gradient estimation is obtained from a HOSM observer after setting the problem into the form of a parameter estimation problem. In contrast with the model-based techniques, the proposed extremum seeking scheme does not require the inclusion of the kinetic model structure in its design. Only some bounds on its curvature are required to guarantee stability. Hence, only a partial model is required, involving only yields and influent substrate concentrations. Moreover, no dither signal is added to the process input like in the perturbation and model-based schemes, instead, it is replaced by the switched nature of the controller with the advantage that the switching action becomes zero in the desired operating point. Another advantage of the HOSM control over the FOSM, like the one in [19], is that the control action (dilution rate) is continuous and hence the chattering, usually associated to this kind of controller, is significantly reduced. Also, the integral term, which is not present in the previous case, allows to reject any constant disturbance. In this work, finite-time stability proofs are also given for the proposed controller (for the first time), first for the nominal case and then considering bounded disturbances. In previous contributions, like [21,22], the stability problem was solved numerically, in this work a Lyapunov function is derived for the HOSM controller. A stable operating region is derived from the stability proofs, and tuning guidelines are given for the case in which an approximate kinetic model is available. The proposed gradient estimation is performed in continuous time rather than with the (slow) sampling time of the controller, like in [17–19]. The advantage in this is that the estimation converges in finite-time and no additional dynamics are added to the closed loop. Another significant difference with many of the works reported in the bibliography is that the proposed control and gradient estimation scheme is based solely in the measurement of cell concentration. This constitutes and advantage in many cases, for example in industrial processes were waste or impure substrates are used. Carbon source or nitrogen on-line measurement may be possible in some cases, but is generally expensive and affine to certain specific substances. On the other hand, cell density can measured by optical density methods or even dielectric spectroscopy in a range of different processes and conditions.

Table 1
Variables and parameters.

Name	Description
x	Cell concentration
s	Substrate concentration
s_f	Fed substrate concentration
v	Volume
D	Dilution rate
y_{xs}	Substrate to biomass yield
μ	Specific growth rate
$\omega(s)$	Gradient of $\mu(s)$ w.r.t. s
$h(s)$	Hessian of $\mu(s)$ w.r.t. s

2. Problem formulation

The model for fed-batch processes in terms of concentrations is obtained from mass balance equations:

$$\dot{x} = (\mu - D)x \tag{1}$$

$$\dot{s} = -\frac{\mu x}{y_{xs}} + D(s_f - s) \tag{2}$$

$$\dot{v} = Dv \tag{3}$$

where all the variables and parameters are referenced in Table 1. It is assumed that an excess of substrate concentration has an inhibiting effect on the specific growth rate, hence, the kinetic of the microorganism is non-monotonic and holds a maximum μ^* at an optimal substrate concentration s^*. It is also assumed that neither the kinetic model or its structure are known, either by uncertainty or lack of identification, therefore the location of the optimal operating point (s^*, μ^*) is unknown.

At this point it is convenient to define some other variables that are important for the proposed control and estimation scheme. Supposing that the specific growth rate is a function of the limiting substrate s only, the gradient of μ can be defined as

$$\nabla\mu = \frac{\partial\mu(s)}{\partial s} = \omega(s), \tag{4}$$

which in this case is scalar because it was supposed that μ depends on a single variable. The gradient is the slope of the kinetic map and indicates the direction in the s axis for which μ increases. Another important variable is the Hessian defined as

$$\nabla^2\mu = \frac{\partial^2\mu}{\partial s^2} = h(s), \tag{5}$$

which is also scalar and describes the curvature of the kinetic map. It is a necessary condition for the the operating point (s^*, μ^*) to be an extreme that $\omega(s^*) = 0$. Particularly, it is a sufficient condition for that point to be a maximum that $h(s^*) < 0$ [23].

Having defined both the gradient $\omega(s)$ and Hessian $h(s)$ of the map (ω and h from now on) it is possible to extend the process

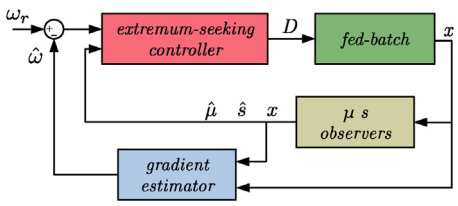

Fig. 1. Control scheme.

model by including the dynamics of μ and ω. By means of the chain rule:

$$\dot{\mu} = \frac{\partial \mu}{\partial s}\dot{s} = \omega\left(-\frac{\mu x}{y_{xs}} + D(s_f - s)\right) \tag{6}$$

$$\dot{\omega} = \frac{\partial \omega}{\partial s}\dot{s} = h\left(-\frac{\mu x}{y_{xs}} + D(s_f - s)\right). \tag{7}$$

Eqs. (6) and (7) are later used to design a gradient estimator to drive the controller and for stability proofs.

The objective in this work is to design a controller capable of driving the specific growth rate to the optimal operating point (s^*, μ^*), which as stated before, is considered unknown. To fulfill the objective a new control and estimation scheme is proposed in this article. A HOSM controller is proposed using an estimation of the gradient as commutation variable and including a term to cancel the natural dynamics of the process. The gradient estimation is obtained with a HOSM observer which uses information of the specific growth rate, substrate concentration and cell concentration as inputs. Previous referenced works using a similar approach consider the substrate concentration as measured variable. In some cases also the gas production rate or some variable that can directly be related to the growth rate. To stay in line with previous contributions and to give a more general framework, in this work it is considered that only the cell concentration can be measured and both the substrate concentration and specific growth rate are estimated from it. Yet, the proposed control and estimation scheme can still be applied if substrate is measured being even easier and more precise.

Remark 1. Cell concentration can be efficiently measured on-line in a number of different scenarios, for low concentrations optical density methods can be used, whereas for high cell concentrations dielectric spectroscopy gives better results, also measuring only viable cells. Substrate concentration is also possible, but sensors are restricted to certain specific substances. Many research lines pursue the conversion of wastes into added value products, where those wastes constitute part of the substrate. In that sense, it seems more feasible to measure cell concentration than the concentration of an impure and non conventional substrate.

3. Extremum seeking controller

The control scheme proposed in this work is depicted in Fig. 1. It is composed of an extremum seeking control algorithm, a gradient estimator and state observers to estimate s and μ. The only measured variables are D and x.

In this section each component of the control scheme is briefly described, while in Section 4 the whole system stability is further analysed along with the tuning of the gains.

3.1. Proposed control law

The proposed controller aims at stabilizing the gradient at a value of $\omega = 0$. The control law is implemented via a HOSM controller:

$$D = \left(\frac{\hat{\mu} x}{y_{xs}} + u_1 + u_2\right)(s_f - \hat{s})^{-1} \tag{8}$$

$$u_1 = k_1 |\hat{\omega}|^{1/2} sign(\hat{\omega}) \tag{9}$$

$$\dot{u}_2 = k_2 sign(\hat{\omega}) \tag{10}$$

where $k_1 > 0$ and $k_2 > 0$ are the design gains, and $\hat{\mu}$ and $\hat{s}$ are estimations of the specific growth rate and substrate concentration, obtained with the observers introduced in Section 3.3. The first term of (8) is a continuous action included to cancel the dynamics of the substrate concentration. It should be noticed that the sliding coordinate is the estimated gradient and that the only measured variable is the cell concentration x.

In the case that all the estimation errors are null, i.e. all the observers converged and $\hat{\mu} = \mu$, $\hat{s} = s$ and $\hat{\omega} = \omega$, and replacing (8) in (2) yields

$$\dot{s} = u_1 + u_2, \tag{11}$$

then the dynamics of the substrate is mostly defined by the sliding mode terms.

The proposed HOSM control law is robust against model uncertainty and disturbances. Moreover, the continuous control action is smoother and produces an inferior magnitude of chattering, mainly because the term (9) becomes zero on the sliding surface ($\hat{\omega} = 0$). Also, the inclusion of the integral term allows rejecting bounded disturbances in the dilution. The stability of the controller and all the aforementioned characteristics rely on the correct tuning of the design gains k_1 and k_2. Stability proofs for the proposed control law and a tuning rule are given in Section 4.

3.2. Gradient estimation

As explained before, the sliding coordinate used by the proposed control law is an estimation of the gradient of the (s, μ) map. From (6) it is observed that ω can be estimated with an observer based estimator if x, μ and s are available for feedback, or at least its estimates. Note that if s is measured, it is even easier to directly estimate $\dot{s}$ without using its model. In order to obtain fast and finite-time convergence of the estimation a HOSM observer is proposed. The classical super-twisting algorithm (STA) [24] is not stable in this case because in (7) the gradient is multiplied by a function which changes its sign throughout the process. For that reason a modified version of the STA is used here, based on the one proposed in [25].

For simplicity $\dot{s}$ is renamed:

$$\dot{s} = -\frac{\mu(s)x}{y_{xs}} + D(s_f - s) = f(\mu, x, s). \tag{12}$$

Then the observer equations are

$$\dot{\eta} = \hat{\omega} f(\hat{\mu}, x, \hat{s}) - \kappa_1 \left| f(\hat{\mu}, x, \hat{s}) \right| |\sigma|^{1/2} sign(\sigma) \tag{13}$$

$$\dot{\hat{\omega}} = -\kappa_2 f(\hat{\mu}, x, \hat{s}) sign(\sigma) \tag{14}$$

$$\sigma = \hat{\mu} - \eta. \tag{15}$$

In this case, η is an auxiliary estimation of the growth rate, $\hat{\omega}$ is the estimation of the gradient and κ_1 and κ_2 are design gains. The sliding coordinate σ is defined as the estimation error of the growth rate made by this observer (when compared to $\hat{\mu}$).

The advantage of this observer based estimator is that a fast and finite-time convergence can be achieved adding no dynamics to the loop in an ideal case. However, some distortion is added by the fact

that the growth rate and substrate concentration signals provided to the estimator are in fact estimations.

3.3. Observers for μ and s

The specific growth rate estimation $\hat{\mu}$ used both by the controller and the gradient estimator is obtained using an exponential observer

$$\dot{\hat{x}} = (\hat{\mu} - D)x - \gamma_1(x - \hat{x}) \tag{16}$$

$$\dot{\hat{\mu}} = \gamma_2 \frac{(x - \hat{x})}{x}, \tag{17}$$

where $\hat{x}$ is the estimation of the (measured) cell concentration. The gains γ_1 and γ_2 can be adjusted to assign the eigenvalues λ_1 and λ_2 of the error dynamics as

$$\lambda_1 + \lambda_2 = \gamma_1 \tag{18}$$

$$\lambda_1 \lambda_2 = \gamma_2. \tag{19}$$

The choice has to be made in such a way that the estimation converges fast but at the same time keeping noise sensitivity low.

On the other hand, the estimation of s is obtained with an asymptotic observer of the form

$$\dot{\hat{z}} = -D(\hat{z} - s_f) \tag{20}$$

$$\hat{s} = \hat{z} - \frac{x}{y_{xs}}. \tag{21}$$

These observers have been extensively treated in the literature, stability proofs and other results can be found in [5]. Alternatively, there are exponential observers based on the measurement of x, such as [26]. However, these require to know if $s > s^*$ or $s < s^*$, which is almost the same thing the gradient estimator tries to determine.

Remark 2. The control algorithm is run with a sampling time large enough to let both the substrate concentration and growth rate show some variation before the next control action is applied. This is one of the key elements that makes the gradient estimation possible in practice. The gradient observer is run at a higher frequency in order to capture those variations and, combined with a proper tuning of the gains, converge fast to the true gradient value. The frequency decoupling resulting from the sampling time differences results in an attenuation of the effect of the estimation errors on the closed loop.

4. Stability analysis

In this section stability proofs are given for the proposed control algorithm. First, in Section 4.1, nominal stability is analysed considering a system without disturbances, i.e. all the estimation errors are null, no model mismatch and no exogenous disturbances. Then, in Section 4.2, practical stability is analysed for a case with bounded disturbances. Differing from previous proposals of the authors where numerical analysis were performed (see [21,22]), analytical stability proofs are given here. A criteria for tuning the controller gains is also derived.

4.1. Nominal stability

First the unperturbed system is considered, thus, no exogenous disturbances, model mismatching or estimation errors are present. The later fact implies that $\hat{\mu} = \mu$, $\hat{s} = s$ and $\hat{\omega} = \omega$. Taking this into account, and replacing (8) in (7) a nominal system is obtained

$$\dot{\omega} = h\left(k_1 |\omega|^{\frac{1}{2}} sign(\omega) + u_2\right) \tag{22a}$$

$$\dot{u}_2 = k_2 sign(\omega) \tag{22b}$$

where h is the (scalar) Hessian of μ, as in (5). The state vector is $y = [\omega, u_2]$ and the equilibrium point is at $y = 0$.

Theorem 1. *The unperturbed system* (22) *converges asymptotically to the origin* $y = 0$ ($\omega = 0, u_2 = 0$) *if the controller gains satisfy*

$$-\frac{2k_2}{k_1^2} > h, \tag{23}$$

were $k_1 > 0$, $k_2 > 0$ *and* $h < 0$.

Proof. First, it should be noted that the right hand sides of the vector field (22) are neither continuous nor locally Lipschitz, thus, the existence of classical solutions cannot be guaranteed [27,Props. 1-2]. However, the existence of unique solutions can be guaranteed for any initial condition in the Filippov sense [27,Prop. 3–5] [28,Ch. 2]. The requirement for the existence of solutions is that the vector field is locally essentially bounded, i.e. bounded on a bounded neighborhood of every point. Then, for every initial condition y_0 the solution is unique if for all y there exists $\varepsilon > 0$ such that the field is essentially one-sided Lipschitz in a ball $B(y, \varepsilon)$. It can be shown that (22) satisfies both conditions, hence, unique solutions exist for every initial condition in the sense of Filippov.

Next, a Lyapunov approach can be taken to show that the origin in (22) is at least asymptotically stable. A quadratic Lyapunov function $V(\xi) = \xi^T P \xi > 0$ can be obtained applying a global homeomorphism, similarly to [29]:

$$\xi_1 = |\omega|^{\frac{1}{2}} sign(\omega) \tag{24}$$

$$\xi_2 = u_2. \tag{25}$$

A new dynamical system is then obtained

$$\dot{\xi}_1 = \frac{1}{2|\xi_1|}(k_1\xi_1 + \xi_2)h \tag{26}$$

$$\dot{\xi}_2 = \frac{1}{2|\xi_1|}(2k_2\xi_1) \tag{27}$$

which can be equivalently rewritten as

$$\dot{\xi} = \frac{1}{2|\xi_1|} A\xi \tag{28}$$

where

$$A = \begin{bmatrix} hk_1 & h \\ 2k_2 & 0 \end{bmatrix}. \tag{29}$$

The eigenvalues of A are located in

$$eigs\{A\} = \frac{hk_1}{2} \pm \sqrt{\left(\frac{hk_1}{2}\right)^2 + 2k_2 h}. \tag{30}$$

Recalling that $k_1 > 0$ and $k_2 > 0$, from the inspection of $eigs\{A\}$ it becomes clear that it is necessary that $\mu(s)$ is convex ($h < 0$) for (28) to be stable.

$$P = \frac{1}{2}\begin{bmatrix} k_1^2 & k_1 \\ k_1 & 2 \end{bmatrix}. \tag{31}$$

Then, in the original domain, the proposed Lyapunov function is:

$$V(y) = V(\omega, u_2) = k_1^2|\omega| + 2k_1 u_2 |\omega|^{\frac{1}{2}} sign(\omega) + 2u_2^2. \tag{32}$$

The proposed $V(y)$ is not Locally Lipschitz continuous at $S = \{(\omega, u_2) \in \mathbb{R}^2 | \omega = 0\}$, hence, the applicability of Lyapunov's theorem [30] is not straightforward. Nevertheless, stability can still be analysed with such non-smooth Lyapunov functions. One approach is given in [27,Theorem 3] by means of the proximal subdifferential of $V(y)$ and and its lower set-valued Lie derivatives. However, in

this case the computation of the proximal subdifferential at S is difficult, mainly because of the lack of convexity of $V(y)$. Alternatively, asymptotic stability can be proven my means of Zubov's theorem [31,Theorem 5,p. 28] [32,Theorem 20.2,p. 568], which states that the origin is asymptotically Lyapunov stable if and only if:

(i) $V(t, y)$ is defined for $||y|| \leq c$ and $t \geq t_0$.
(ii) $V(t, 0) = 0 \forall t \geq t_0$ and is continuous in $y \forall t \geq t_0$ in the point $y = 0$.
(iii) $V(t, y)$ is positive definite.
(iv) $V(t, y)$ decreases monotonically to the origin.

The proposed Lyapunov function clearly satisfies conditions i to iii, then, it only rests to show that $V(y)$ decreases along the trajectories of (22). This can be answered in terms of [33,Lemma 6.1], if $V(\varphi(t, y_0))$ is absolutely continuous and $\dot{V}(\varphi(t, y_0)) < 0$ almost everywhere, then $V(\varphi(t, y_0))$ is non increasing. Since both $\varphi(t, y_0)$ and $V(y)$ are absolutely continuous functions, then, its composition $V \circ \varphi(t, y_0)$ is absolutely continuous only if $\varphi(t, y_0)$ is monotone [34]. To prove that $\varphi(t, y_0)$ is monotone, suppose that $\varphi_2(t, y_0) \neq 0$ when crossing $\varphi_1(t, y_0) = 0$ at an instant $t = \tau$. As $\dot{\omega} = h\left(k_1|\omega|^{\frac{1}{2}} sign(\omega) + u_2\right)$, during a time interval containing τ, $\varphi_1(t, y_0)$ can either increase or decrease monotonically. In the case that $\varphi_2(t, y_0) = 0$ and $\varphi_1(t, y_0) = 0$, the origin is reached and $\varphi_1(t, y_0)$ will stay zero [29].

Next, we show that $\dot{V}(y)$ is negative definite almost everywhere. Differentiating $V(\xi)$ with respect to time yields

$$\dot{V} = -\frac{1}{2|\xi_1|}\xi^T Q \xi \tag{33}$$

where

$$Q = -(A^T P + PA) = \\ = \begin{bmatrix} -hk_1^3 - 2k_1k_2 & -hk_1^2 - 2k_2 \\ -hk_1^2 - 2k_2 & -hk_1 \end{bmatrix} \tag{34}$$

and

$$\det\{Q\} = -2hk_1^2k_2 - 4k_2^2 \tag{35}$$

As before, if $k_1 > 0$ and $k_2 > 0$, $h < 0$ is necessary for $Q > 0$. From (34) and (35), setting both the upper left minor and the determinant greater than zero, the condition

$$-\frac{2k_2}{k_1^2} > h \tag{36}$$

is obtained. □

Theorem 1 states that stability is guaranteed only for sufficiently negative values of the Hessian, i.e. sufficiently far from inflexion points. The boundary surface defined by (23), defined from now on as $\underline{h} = -2k_2/k_1^2$, is depicted in Fig. 2(a) and some contour lines in Fig. 2(b). This bound represents the value of h closest to zero admissible to assure stability. In other words, is the smallest value that the curvature of $\mu(s)$ can have. It becomes clear from both figures that lower k_1 values result in $\underline{h}$ farther from zero, thus reducing the stability region. It can also be noticed that when $k_2 \to 0$, the bound for the Hessian relaxes as $\underline{h} \to 0$.

Theorem 2. *System (22) achieves finite-time convergence, with convergence time bounded by:*

$$T \leq \frac{4\lambda_{\max}\{P\}}{\lambda_{\min}\{P\}\lambda_{\min}\{Q(h)\}} V(0)^{1/2}. \tag{37}$$

Proof. From the fact that

$$||\xi||^2\lambda_{\min}\{Q(h)\} < \xi^T Q(h)\xi < ||\xi||^2\lambda_{\max}\{Q(h)\},$$

and from (33):

$$\dot{V} \leq -\frac{1}{2|\xi_1|}\lambda_{\min}\{Q\}||\xi||^2. \tag{38}$$

Then, as $|\xi_1| \leq ||\xi||$ and

$||\xi||^2\lambda_{\min}\{P\} < V < ||\xi||^2\lambda_{\max}\{P\}$:

$$\dot{V} \leq -\frac{\lambda_{\min}\{P\}\lambda_{\min}\{Q(h)\}}{2\lambda_{\max}\{P\}} V^{1/2}. \tag{39}$$

The solution to the differential equation $\dot{v} = -cv^{1/2}$, where c is a constant, is

$$v(t) = \left(v(0)^{1/2} - \frac{c}{2}t\right)^2. \tag{40}$$

Then, by comparison [30]

$$V(t) \leq \left(V(0)^{1/2} - \frac{\lambda_{\min}\{P\}\lambda_{\min}\{Q(h)\}}{4\lambda_{\max}\{P\}}t\right)^2. \tag{41}$$

Finally, the time for which $V(t)$ extinguishes is bounded by

$$T \leq \frac{4\lambda_{\max}\{P\}}{\lambda_{\min}\{P\}\lambda_{\min}\{Q(h)\}} V(0)^{1/2}. \tag{42}$$

□

4.2. Practical stability

Previously, the stability of the unperturbed system (22) was analysed. Consider now the perturbed system:

$$\dot{\omega} = h\dot{s} = h\left(k_1|\omega|^{\frac{1}{2}} sign(\omega) + u_2 + \rho_1\right) \tag{43a}$$

$$\dot{u}_2 = k_2 sign(\omega) + \rho_2 \tag{43b}$$

where ρ_1 and ρ_2 are the disturbance terms. The source of these disturbances can be external to the system, model mismatching or estimation errors produced by the auxiliary observers. The last two sources are closely related, since persistent estimation errors generally arise from model uncertainty.

Consider now the class of disturbances that can be bounded by

$$|\bar{h}\rho_1| \leq \delta_1 \quad |\rho_2| \leq \delta_2 \tag{44}$$

where $\delta_1 \geq 0$ and $\delta_2 \geq 0$ are constants and $\bar{h} < 0$ is a lower bound for the Hessian function.

Under this class of disturbances, practical stability [35] can be obtained in terms of the following theorem:

Theorem 3. *System (43) is practically stable if the disturbances can be bounded as in (44) and*

$$\delta_2 < \frac{\lambda_{\min}\{Q\}}{4\lambda_{\max}\{P\}} \quad \forall \delta_1 \geq 0, \tag{45}$$

were $\lambda_{\min}\{Q\}$ and $\lambda_{\max}\{P\}$ are the minimum and maximum eigenvalues of Q and P respectively. Moreover, the convergence time is bounded by

$$T \leq \frac{\lambda_{\max}\{P\}^{\frac{1}{2}}}{\epsilon\left(\frac{1}{2}\lambda_{\min}\{Q\} - 2\delta_2\lambda_{\max}\{P\}\right)}. \tag{46}$$

Theorem 3 is similar to one given in [36], but with the difference that here matrix Q is not constant but depends on the variable h. This comes from (43a) where h multiplies all the terms in the equation.

Proof. First, coordinate change (26) and (27) is applied to the disturbed system (43), giving place to

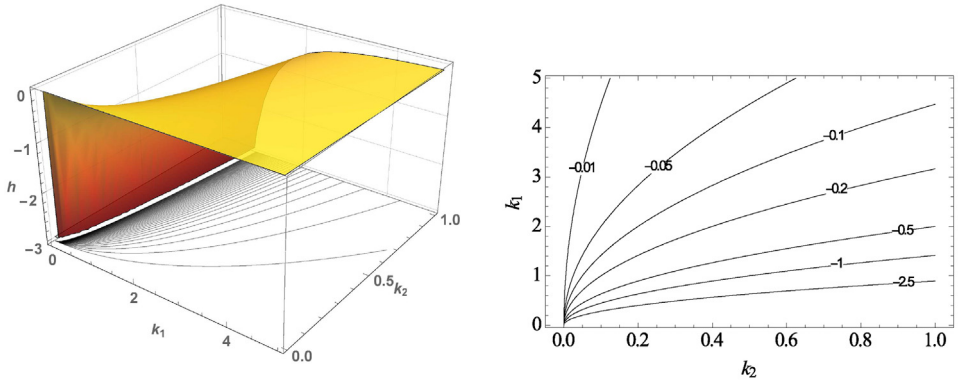

(a) Surface showing for each pair of gains the maximum hessian that the kinetic model can have for which stability is guaranteed

(b) Minimum pair of gains that guarantee stability for different values of the maximum hessian

Fig. 2. Hessian bounds for nominal stability.

$$\dot{\xi} = \frac{1}{2|\xi_1|}\left(A\xi + \varrho_1\right) + \varrho_2 \tag{47}$$

where matrix A is h dependent (see (29)) and the disturbance vectors are

$$\varrho_1 = \begin{bmatrix} h\rho_1 \\ 0 \end{bmatrix} \quad \varrho_2 = \begin{bmatrix} 0 \\ \rho_2 \end{bmatrix}. \tag{48}$$

With this structure in mind, the same Lyapunov function of the nominal case $V(\xi) = \xi^T P\xi$ is proposed (the same considerations as in the nominal case are made regarding the lack of Lipschitzness of V). In the disturbed case, its derivative is

$$\dot{V} = -\frac{1}{2|\xi_1|}\left(\xi^T Q\xi - \varrho_1^T P\xi\right) + 2\varrho_2^T P\xi \tag{49}$$

Then, if (45) holds, $\dot{V}$ can be bounded as

$$\begin{aligned} \dot{V} &\leq -\epsilon \frac{\frac{1}{2}\lambda_{\min}\{Q\} - 2\delta_2\lambda_{\max}\{P\}}{\frac{1}{2}\lambda_{\max}\{P\}} V \frac{1}{2}, \\ \forall ||\xi||_2 &> \frac{\delta_1\lambda_{\max}\{P\}}{2(1-\epsilon)\left(\frac{1}{2}\lambda_{\min}\{Q\} - 2\delta_2\lambda_{\max}\{P\}\right)} = r, \\ 0 &< \epsilon < 1. \end{aligned} \tag{50}$$

The details on how to obtain (50) from (49) are not given due to its length. However, although in this case Q is not a constant matrix as in the case developed in [36], the mathematical steps for the deduction are the same.

Matrix Q is symmetric and positive definite but also depends on h, then, its eigenvalues λ_{Qi} are real, positive and also depend on h:

$$\lambda_{Qi} = -h\frac{k_1}{2}(1+k_1^2) - k_1k_2 \pm \left(ah^2 + bh + c\right)^{\frac{1}{2}} \tag{51a}$$

$$a = \frac{k_1^2}{4}(1 + 2k_1^2 + k_1^4) \tag{51b}$$

$$b = k_1^2k_2(3 + k_1^2) \tag{51c}$$

$$c = k_2^2(4 + k_1^2). \tag{51d}$$

For that reason, the minimum eigenvalue of Q must then be found by minimizing the above expression (with the minus sign before the square root) with respect to h restricted to an interval $(\bar{h}, \underline{h})$, where $\bar{h} < \underline{h} < 0$, $\underline{h}$ is obtained from (23) and $\bar{h}$ can be obtained from the kinetic model, if available, as the smallest possible Hessian for that growth rate kinetics.

The result in (50) assures that the trajectories of system (43) converge to a ball of radius r around the origin in finite-time. In the case that $\rho_1 = 0$ and $\rho_2 \neq 0$ the radius of the ball is zero for any finite δ_2. In the case that $\rho_1 \neq 0$ and $\rho_2 = 0$ the ball will have a radius different than zero. However, inspecting (43) it can be observed that in that case the only equilibrium point is $\omega = 0$, $u_2 = -\rho_1$, then, if practical stability holds convergence will be to that unique equilibrium point. Particularly, note that the coordinate change ξ could be redefined with $\xi_2 = u_2 + \rho_1$, then

$$\dot{\xi}_2 = k_2 sign(\hat{\omega}) + \dot{\rho}_2. \tag{52}$$

If ρ_2 is constant the same proof for nominal stability shows that $y = [0, -\rho_2]$ is finite time stable. Otherwise, convergence to that point depends on the tuning of the gains so that Theorem 3 holds (and also, from (52), that $k_2 > \max|\dot{\rho}_2|$). Finally, in the case that $\rho_1 \neq 0$ and $\rho_2 \neq 0$, only convergence to a neighborhood of the origin can be guaranteed. For example, suppose that $\hat{\omega} \neq \omega$, the controller would drive the system to $\hat{\omega} = 0$ (from replacing (8) in (7)). That is equivalent to having an error in the measurement (of ω for instance), which would inevitably make the system converge to a point different than the origin. Practical stability guarantees finite-time convergence to a given region related to that error. Moreover, since the observers for μ and s have an asymptotic convergence, the closed loop convergence rate will be dominated by them, i.e. the gradient will converge in finite-time to a value with an error and from there asymptotically to the origin. Of course, in cases where both the substrate concentration and the growth rate can be measured, such as anaerobic digestion [17,19], this limitation is not present.

Remark 3. For the system under study, many kind of disturbances fit in the class defined in (44). First, as many observers are involved in the loop, estimation errors are an evident source of perturbation. Second, there are disturbances caused by the uncertainty in the model parameters used in the algorithms, in this case s_f and y_{xs}, which at the same time causes estimation errors. Both, the estimation and model parameter errors are usually bounded. For example, the growth rate estimation error $0 < \tilde{\mu} < \mu^{\max}$. Similarly, the substrate concentration will be known in general with a certain precision given by a weighting device. Then, it can be shown that the produced disturbances can also be bounded by a constant.

Measurement noise can be handled as other kind of disturbances if it can be bounded in the same way. For example, normally distributed noise with zero mean can be bounded to three standard deviations in a practical sense. In this work, only biomass is measured and care must be taken on how noise propagates though the observer algorithms. Both the exponential observer for growth rate estimation and the sliding mode observer for gradient estimation can keep noise levels attenuated with a proper choice of gains [5,25]. On the other hand, the noise attenuation by the asymptotic observer cannot be controlled easily. In general, it should be checked that the signal to noise ratio for substrate is sufficiently high. Also, $s_f >> s$ should always hold to keep the denominator $s_f - s$ in (8) far from zero.

4.3. Additional comments on stability

A possible scenario is that $\lambda_{\min}\{Q\} = 0$, which is the case when $\underline{h} = \frac{-2k_2}{k_1^2}$. For that reason, some stability margin should be taken in the design in order to obtain $\lambda_{\min}\{Q\} > 0$ strictly. Going back to (34), the stability condition can be set to

$$Q = (-A^T P + PA) > 2\alpha P. \tag{53}$$

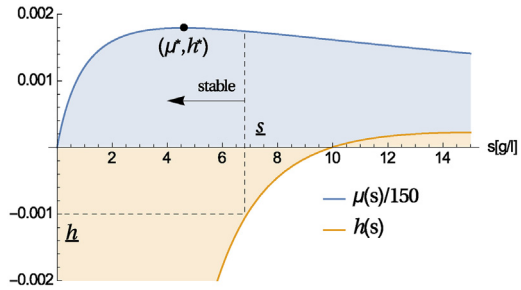

Fig. 3. Kinetic model and Hessian used in the simulations.

This is a standard decay rate problem, if $P > 0$ exists, the eigenvalues of A are $eigs\{A\} < -\alpha$. Moreover, the eigenvalues of Q are $eigs\{Q\} > 2\alpha\lambda_{\min}\{P\}$. From (34), (31) and (53) conditions for the gains can be obtained.

Theorem 4. *It is a sufficient condition for* $eigs\{Q\} > 2\alpha\lambda_{\min}\{P\}$ *that the controller gains satisfy*

$$h < \frac{-\alpha k_1 - 2k_2}{k_1^2} \tag{54}$$

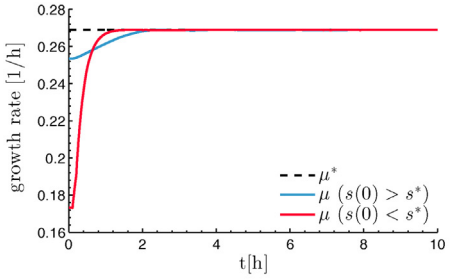

(a) Specific growth rate.

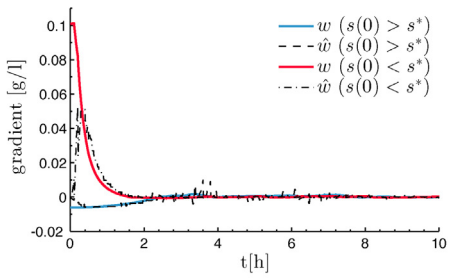

(b) Gradient and estimation

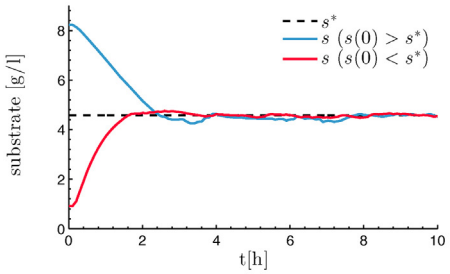

(c) Substrate concentration.

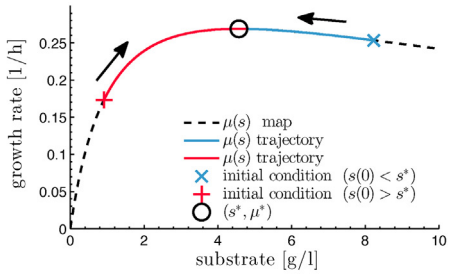

(d) Substrate concentration and specific growth rate map.

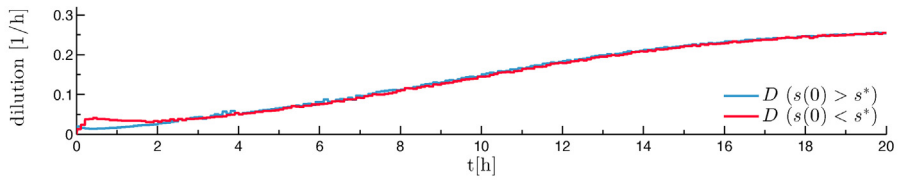

(e) Dilution rate.

Fig. 4. Simulation results for the control and estimation scheme starting from different initial conditions for the substrate. Red line: Initial substrate concentration below the optimal value. Blue line: Initial substrate concentration above the optimal value. (For interpretation of the references to color in this figure legend, the reader is referred to the web version of this article.)

$$h < -\frac{2\alpha}{k_1}. \tag{55}$$

Under these conditions the convergence time is bounded by

$$T \leq \frac{2\lambda_{\min}\{P\}^{\frac{1}{2}}}{\alpha} V(0)^{1/2}, \tag{56}$$

which does not depend on the Hessian h.

Proof. From (53) the stability condition is equivalent to $-M = A^T P + PA + 2\alpha P < 0$, then

$$M = \begin{bmatrix} -k_1(\alpha k_1 + hk_1^2 + 2k_2) & -(\alpha k_1 + hk_1^2 + 2k_2) \\ -(\alpha k_1 + hk_1^2 + 2k_2) & -(2\alpha + hk_1) \end{bmatrix} > 0. \tag{57}$$

Then, by solving the inequalities for all the principal minors of M conditions (54) and (55) are obtained.

$$-\frac{1}{2|\xi_1|}\xi^T Q \xi < -\frac{\alpha}{|\xi_1|} V. \tag{58}$$

Then, as

$$|\xi_1| \leq ||\xi|| < \frac{V^{\frac{1}{2}}}{\lambda_{\min}\{P\}^{\frac{1}{2}}}$$

it can be shown that

$$\dot{V} < -\frac{\alpha}{\lambda_{\min}\{P\}^{\frac{1}{2}}} V^{\frac{1}{2}}. \tag{59}$$

Then, as shown in Section 4.1 (56) is obtained. □

Remark 4. The stability domain is initially defined by the ratio $-2k_2/k_1^2$ as stated in (23), which sets a lower bound for the curvature of the kinetics (the largest negative Hessian $\underline{h}$). To strengthen stability, more strict conditions are defined in (54) and (55). Based on these conditions a tuning approach can be derived for cases when an approximate kinetic model is available:

1. Differentiate $\mu(s)$ twice w.r.t. s to obtain the Hessian $h(s)$.
2. Find lower and upper bounds for $h(s)$, if for some values of s $h(s) \geq 0$ define a maximal substrate concentration $\underline{s}$ such that $h(\underline{s}) = \underline{h} < 0$.
3. Define a value for α.
4. Find k_1 and k_2 such that both $\frac{-\alpha k_1 - 2k_2}{k_1^2} > \underline{h}$ and $-\frac{2\alpha}{k_1} > \underline{h}$ hold.
5. If the obtained gains are too large or the problem is infeasible repeat defining either a smaller α or a smaller $\underline{s}$.

5. Simulation results

In this section simulation results for the proposed extremum seeking controller and gradient estimation are shown under different scenarios. The process to be controlled is described by (1)–(3). The specific growth rate kinetic model used for the simulations is similar to the one presented in [37,38] for the growth stage of a PHB production process:

$$\mu = \frac{\mu_{\max} s}{k_s + s + \frac{s^2}{k_i}}. \tag{60}$$

The values for the model parameters and other parameters of the process are: $\mu_{\max} = 0.41\ \text{h}^{-1}$, $k_s = 1.2$ g/L, $k_i = 17.43$ g/L, $s_f = 200$ g/L, $y_{xs} = 0.48$ g/g. Also, the optimal substrate concentration and growth rate are $s^* \cong 4.6$ g/L and $\mu^* \cong 0.27$ 1/h.

The specific growth rate observer gains used are $\gamma_1 = -40$ and $\gamma_2 = 400$ to ensure a fast convergence and tracking. The gradient estimator gains where adjusted as $\kappa_1 = 4.5$ and $\kappa_2 = 10$. The controller gains are $k_1 = 20$ and $k_2 = 0.2$, which from (23) give a maximum bound for the Hessian $\underline{h} \cong -0.001$ which corresponds to a substrate concentration $\underline{s} \cong 7$ g/L. The minimum eigenvalue of Q for $h < \underline{h}$ is zero exactly when $h = \underline{h}$. In order to obtain a $\lambda_{\min}\{Q(h)\} > 0$, (54) and (55) can be used with $\alpha = 0.01$ and the previous gains, obtaining a new bound $\underline{h} = -0.0015$, thus slightly reducing the stability region. Fig. 3 shows the specific growth rate and Hessian values with respect to the substrate concentration ($\mu(s)$ attenuated 150 times to show them in the same graph). The stability region is marked with dashed lines.

The first scenario, shown in Fig. 4, depicts the controller and estimator response when starting with two different initial conditions for the substrate. The curves in blue correspond to the case of an initial substrate concentration higher than the optimal ($s(0) = 8.2$ g/L), the curves in red correspond to an initial condition lower than the optimal ($s(0) = 0.9$ g/L). Both initial conditions are equidistant from the optimum, and notice that the high one is even outside the stability region. Regarding the growth rate and substrate observers, in this scenario both are started with no estimation error. In Fig. 4(a) it can be seen that the specific growth rate reaches the optimal value in approximately 2 hours. The same can be observed with the substrate concentration in Fig. 4(c). Fig. 4(b) shows the gradient ω and its estimation $\hat{\omega}$ for the two cases, where it can be first noticed a fast convergence of the estimates in less than an hour and how the gradient converges to zero due to the control action which is shown in Fig. 4(e). The small errors present in the gradient estimation are originated by the delays in the growth rate observer, which has been tuned keeping a balance between convergence speed and noise rejection. Finally Fig. 4(d) shows the growth rate trajectory in the (s, μ) plane where the convergence to the maximum rate can be observed clearly.

Fig. 5 shows the scenario in which the specific growth rate and substrate observers are started with some error. In the case of the growth rate the error is 50% and in the case of the substrate 200% as it can be observed in Fig. 5(a) and (b). The growth rate estimation has a fast convergence in accordance to the selected gains γ_1 and γ_2. On the other hand, the substrate estimation does not converge rapidly because its convergence rate depends on the dilution rate. However, this does not have a significant effect on the gradient estimation because it is its derivative $\dot{\hat{s}} = -\hat{\mu}x/y_{xs} + D(s_f - s)$ which affects the estimation rather than its instantaneous value (see (12) and (13)), and since $s_f >> s$ it can be concluded that the $\hat{s}$ is not significantly affected by errors in $\hat{s}$. Fig. 5(c) shows the gradient and its estimation, where it can be observed that although there is a large undershoot at the beginning (mostly because the specific growth rate estimation error), convergence is still fast.

The next scenario consists in testing the control and gradient estimation with a slowly time varying optimum and is depicted in Fig. 6. The variation in μ^* is produced by introducing an additional factor in the kinetic model dependent on a second substrate, nitrogen n in this case, as in [37,38]. Then, the kinetic model is

$$\mu = \frac{\mu_{\max} s}{k_s + s + \frac{s^2}{k_i}} \cdot \frac{n}{k_n + n + \frac{n^2}{k_{in}}}, \tag{61}$$

where $\mu_{\max} = 0.745$, $k_n = 5$, $k_{in} = 30$, k_s and k_i are the same as before. With the new factor s^* remains the same and μ^* will vary depending on the nitrogen concentration. The two substrates are added together with the same flow rate, the fed concentration for the second is $n_f = 40$ g/l which results in a slow accumulation of it. As shown in Fig. 6(b), the worst effect of the varying optimum appears in the gradient estimation because a disturbance term appears in (4):

$$\dot{\mu} = \omega \dot{s} + \frac{\partial \mu}{\partial n} \dot{n} = \omega \dot{s} + \phi \tag{62}$$

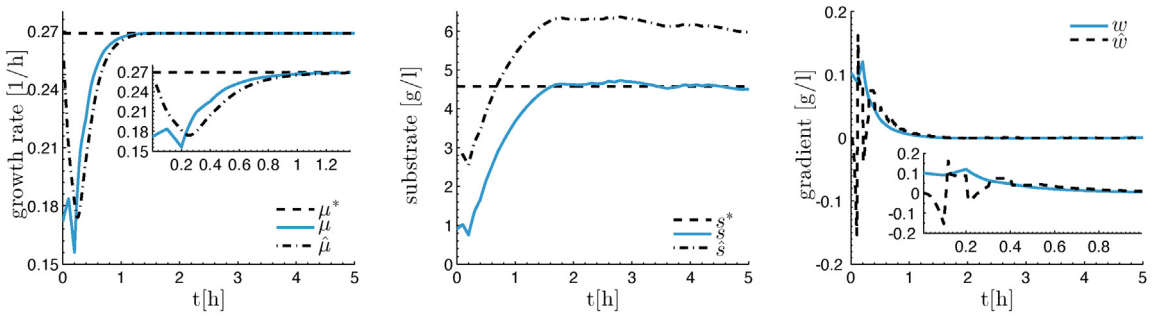

(a) Specific growth rate and estimation. **(b)** Substrate concentration and estimation. **(c)** Gradient and estimation

Fig. 5. Simulation results for the control and estimation scheme when the observers initial conditions have errors. Solid lines: Real values. Dot-dashed lines: Estimated values. Dashed lines: Optimal values.

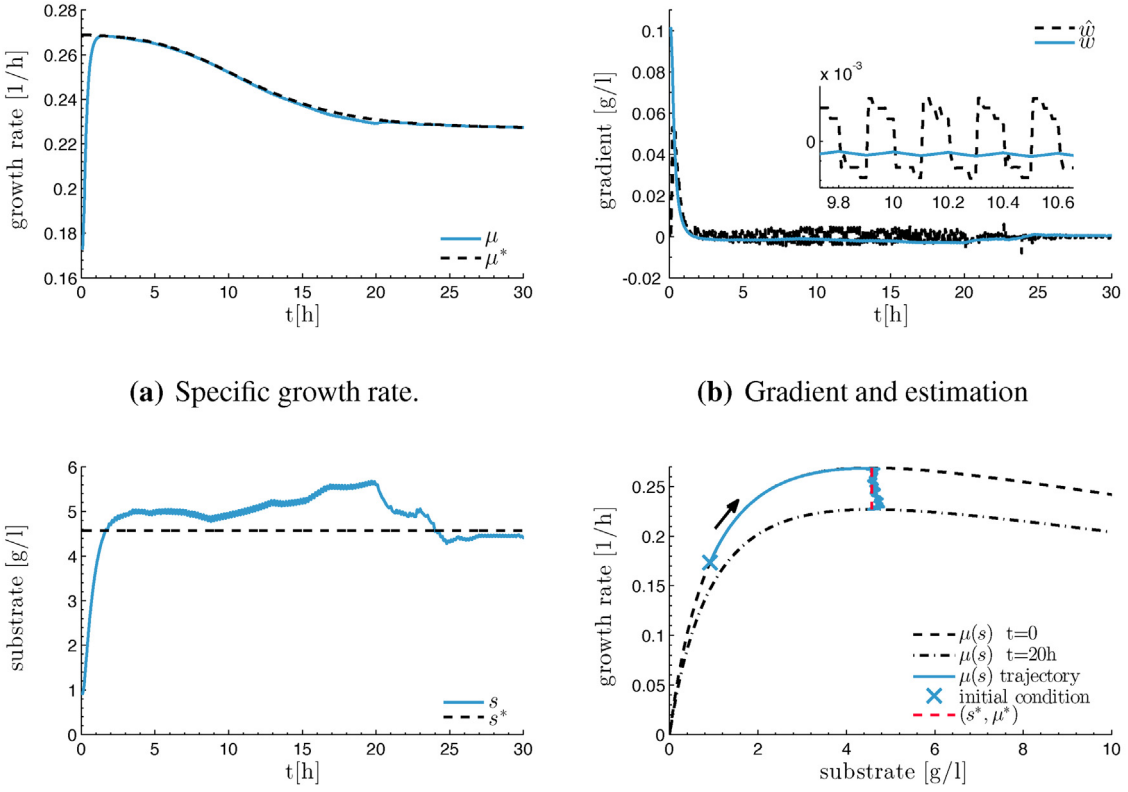

(a) Specific growth rate. **(b)** Gradient and estimation

(c) Substrate concentration. **(d)** Substrate concentration and specific growth rate map.

Fig. 6. Simulation results for the control and estimation scheme with a time varying optimum. Blue line: True values. Dashed line: (a) and (c) optimal values, (b) estimated gradient, (d) initial map. Dot-dashed line: (d) final map. (For interpretation of the references to color in this figure legend, the reader is referred to the web version of this article.)

where ϕ is the disturbance term capturing the variations in μ produced by n. The growth rate estimation error can be obtained by subtracting the previous equation to (13)

$$\dot{\tilde{\mu}} = \dot{\sigma} = \dot{\mu} - \dot{\eta} = \tilde{\omega}\dot{s} + \phi - \kappa_1 \left|\dot{s}\right| |\sigma|^{1/2} sign(\sigma), \tag{63}$$

then, when the equilibrium has been reached ($\dot{\sigma} = \sigma = 0$)

$$\tilde{\omega} = -\frac{\phi}{\dot{s}}. \tag{64}$$

First, it should be noted that the discrete operation of the controller makes $\dot{s} \neq 0$ most of the time as it can be observed in Fig. 6(c) where s presents a small ripple. Secondly, the disturbance ϕ should not be high to assure a small error in the gradient estimation, which means that either the slope $\frac{\partial \mu}{\partial n}$ is small, which is a valid assumption if n is not the limiting substrate, or the rate of change $\dot{n}$ is small. This is illustrated at times 10–20 h where the substrate concentration is farther from its optimum value and the specific growth rate change

is the fastest. The gradient estimation is depicted in Fig. 6(b), it can be observed that despite the errors the estimation still stays around a neighborhood of the real value. The small box shows the detail of the estimation, note that the steps correspond to the sign changes in $\dot{s}$. If ϕ was faster some steady state error would appear both in s and $\hat{\omega}$ due to the fact that all the changes in μ would be attributed to the changes in s only. Finally, Fig. 6(d) shows the trajectory in the (s, μ) space, the initial and final kinetic models are included (black dashes and black dot-dashes respectively) as well as the trajectory of the optimal (s^*, μ^*) (red dashes). It can be observed a good tracking of the optimal point.

In the last scenario noise is added to the cell density measurement and is depicted in Fig. 7. White noise with variance $\sigma^2 = 0.1$ is used, filtered in the range of 240–1000 h^{-1} (~0.07–0.3 Hz). The eigenvalues of the specific growth rate observer (16) and (17) increase their magnitude as cells grow, as described in (18) and (19). The results for the growth rate and its estimation are presented in Fig. 7(a), were it can be observed that although the tracking is degraded by noise, as cell density increases the noise in the estimation decreases, which can be related to the increase in the signal to noise ratio of the measurement. The substrate and its estimation are plotted in Fig. 7(b), where it can be observed that in this case the noise gain is constant throughout the experiment due to the use of the asymptotic observer. It is this noise in a great deal combined to the noise in specific growth rate estimation that degrades the gradient estimation and consequently the control loop performance, as shown in Fig. 7(c). The interpretation is simple: the gradient estimation relies on observing changes in μ and s, if those changes have the same magnitude as the noise the gradient estimator will not be able to distinguish real variations from the ones produced by noise. In the simulated case the control objective is still achieved since the growth rate reaches and stays in the maximum. However, in scenarios where the noise conditions are more severe, an easy solution is to decrease the controller sampling time, in that way the variations in the substrate become larger and more distinguishable from the noise.

6. Discussion and conclusions

The proposed control and estimation scheme was tested under many scenarios including imperfect initial conditions in the estimations, measurement noise and a time varying optimal operating point. In all the scenarios the control objective of reaching the unknown maximum specific growth rate is achieved in a short time and the stability conditions obtained in Section 4 are verified. Unlike previous referenced extremum seeking schemes based on the use of dither signals or on first order sliding modes, the growth rate response is smooth and the oscillations or chattering after convergence are almost negligible. The later fact is in line with the utilization of a HOSM control with the discontinuity in the derivative of the control action. Moreover, it was shown that the integral action allows rejecting bounded disturbance in the process input. With respect to the gradient estimation, the proposed observer verifies the convergence and robustness properties of a super-twisting algorithm. It shows to be a valid alternative to other estimators proposed in the literature with the advantage that no dynamics are added to the loop and a perfect tracking can be obtained in ideal conditions. From the results it can be derived that the controller performance is strongly linked to the accuracy of the gradient estimator. Both in the case with noisy measurements and the case

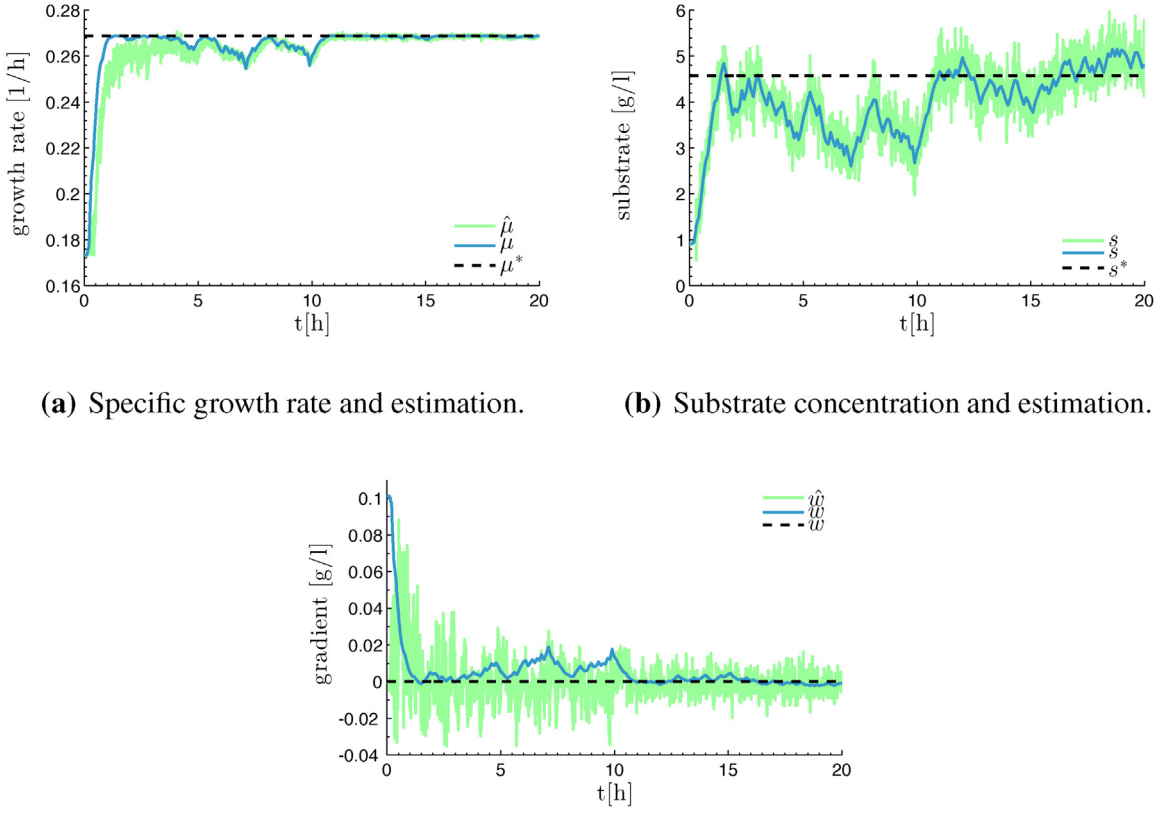

(a) Specific growth rate and estimation.

(b) Substrate concentration and estimation.

(c) Gradient and estimation

Fig. 7. Simulation results for the control and estimation scheme under measurement noise conditions. Blue lines: Real values. Green lines: Estimations. Dashed line: Optimal values. (For interpretation of the references to color in this figure legend, the reader is referred to the web version of this article.)

with a varying optimum the results show that despite the maximum growth rate is reached, the substrate concentration tracking is affected. In the fist case it is mostly attributed to the corrupted growth rate and substrate estimations, but in the second case it is because the estimator interprets that the only factor influencing the growth rate is the substrate, hence driving the substrate to a different value than s^*. However, as long as the factors influencing μ do not produce fast or large variations and the algorithms are properly tuned, the results verify that the control objective is accomplished.

In most reported bioprocess extremum seeking works the measurement of substrate concentration is used, in this work the variables fed to the controller algorithm are obtained from the measurement of cell density. In our view this is an advantage in many biotechnological processes, such as those which involve waste treatment or conversion and whose research is being encouraged worldwide. These kind of processes are not fed with pure substrates which makes substrate measurement not always possible. Optical density and dielectric spectroscopy are feasible monitoring methods for these processes. Alternatively, gas phase measurements can be used when available, as in [19,17]. Nevertheless, the same proposed controller and gradient estimator can be adapted if other measurements are available as long as reliable growth rate, substrate and cell density information can be obtained. Another point to highlight is that waste processes may not be easy to characterize, in that sense, the proposed control scheme does not require the knowledge of the kinetic model parameters or its structure.

One of the factors influencing the gradient estimation accuracy are the estimation errors in the specific growth rate and substrate, for that reason, in future work the extremum seeking scheme will be tested using alternative observers for μ and s, particularly sliding model algorithms in an attempt to obtain faster estimates and reduce the effect of noise.

Acknowledgements

This work was supported by the Agencia Nacional de Promoción Científica y Tecnológica, Argentina, PICT 2014-2394; CONICET, Argentina, PIP 112-201501-00837; We would also like to acknowledge Universidad Nacional de La Plata.

References

[1] E. Picó-Marco, J. Navarro, J. Bruno-Barcena, A closed loop exponential feeding law: invariance and global stability analysis, J. Process Control 16 (4) (2006) 395–402, http://dx.doi.org/10.1016/j.jprocont.2005.06.014.
[2] M. Dabros, M. Schuler, I. Marison, Simple control of specific growth rate in biotechnological fed-batch processes based on enhanced online measurements of biomass, Bioprocess Biosyst. Eng. 33 (9) (2010) 1109–1118, http://dx.doi.org/10.1007/s00449-010-0438-2.
[3] R. Biener, A. Steinkämper, T. Horn, Calorimetric control of the specific growth rate during fed-batch cultures of *Saccharomyces cerevisiae*, J. Biotechnol. 160 (3–4) (2012) 195–201, http://dx.doi.org/10.1016/j.jbiotec.2012.03.006.
[4] I.Y. Smets, G.P. Bastin, J.F. Van Impe, Feedback stabilization of fed-batch bioreactors: non-monotonic growth kinetics, Biotechnol. Prog. 18 (5) (2002) 1116–1125, http://dx.doi.org/10.1021/bp010191p.
[5] G. Bastin, D. Dochain, On-Line Estimation and Adaptive Control of Bioreactors, Process Measurement and Control, Elsevier, Amsterdam, 1990, http://dx.doi.org/10.1016/B978-0-444-88430-5.50001-3.
[6] I. Cornet, D. Dochain, B. Ramsay, J. Ramsay, M. Perrier, Application of an adaptive linearizing inferential controller to a PHB process, Biotechnol. Biotechnol. Equip. 9 (1) (1995) 96–102, http://dx.doi.org/10.1080/13102818.1995.10818832.
[7] D. Dochain (Ed.), Bioprocess Control, ISTE Wiley, London Hoboken, NJ, 2008.
[8] E. Picó-Marco, J.P. Picó, H.D. Battista, Sliding mode scheme for adaptive specific growth rate control in biotechnological fed-batch processes, Int. J. Control 78 (2) (2005) 128–141, http://dx.doi.org/10.1080/00207170500007372.
[9] H. De Battista, J. Picó, E. Picó-Marco, Nonlinear {PI} control of fed-batch processes for growth rate regulation, J. Process Control 22 (4) (2012) 789–797, http://dx.doi.org/10.1016/j.jprocont.2012.02.011.
[10] D. Dochain, M. Perrier, M. Guay, Extremum seeking control and its application to process and reaction systems: a survey, Math. Comput. Simul. 82 (3) (2011) 369–380, http://dx.doi.org/10.1016/j.matcom.2010.10.022, 6th Vienna International Conference on Mathematical Modelling.
[11] K. Ariyur, M. Krstic, Real Time Optimization by Extremum Seeking Control, Wiley Interscience, Hoboken, NJ, 2003.
[12] H.-H. Wang, M. Krstić, G. Bastin, Optimizing bioreactors by extremum seeking, Int. J. Adapt. Control Signal Process. 13 (8) (1999) 651–669, http://dx.doi.org/10.1002/(SICI)1099-1115(199912)13:8<651::AID-ACS563>3.0.CO;2-8.
[13] M.T. Angulo, Nonlinear extremum seeking inspired on second order sliding modes, Automatica 57 (2015) 51–55, http://dx.doi.org/10.1016/j.automatica.2015.04.001.
[14] P. Cougnon, D. Dochain, M. Guay, M. Perrier, On-line optimization of fedbatch bioreactors by adaptive extremum seeking control, J. Process Control 21 (10) (2011) 1526–1532, http://dx.doi.org/10.1016/j.jprocont.2011.05.004, Special Issue: Selected Papers From Two Joint {IFAC} Conferences: 9th International Symposium on Dynamics and Control of Process Systems and the 11th International Symposium on Computer Applications in Biotechnology, Leuven, Belgium, July 5–9, 2010.
[15] B. Daaou, D. Dochain, High order sliding mode observer based extremum seeking controller for a continuous stirred tank bioreactor, 2015 3rd International Conference on Control, Engineering Information Technology (CEIT) (2015) 1–6, http://dx.doi.org/10.1109/CEIT.2015.7233018.
[16] N. Marcos, M. Guay, D. Dochain, T. Zhang, Adaptive extremum-seeking control of a continuous stirred tank bioreactor with Haldane's kinetics, J. Process Control 14 (3) (2004) 317–328, http://dx.doi.org/10.1016/S0959-1524(03)00070-2.
[17] A. Vargas, J.A. Moreno, On-line maximization of biogas production in an anaerobic reactor using a pseudo-super-twisting controller, IFAC-PapersOnLine 48 (8) (2015) 14–19, http://dx.doi.org/10.1016/j.ifacol.2015.08.150, 9th {IFAC} Symposium on Advanced Control of Chemical Processes {ADCHEM} 2015 Whistler, Canada, June 7–10, 2015.
[18] A. Vargas, J. Moreno, A.V. Wouwer, Super-twisting estimation of a virtual output for extremum-seeking output feedback control of bioreactors, J. Process Control 35 (2015) 41–49, http://dx.doi.org/10.1016/j.jprocont.2015.08.003.
[19] G. Lara-Cisneros, R. Femat, D. Dochain, An extremum seeking approach via variable-structure control for fed-batch bioreactors with uncertain growth rate, J. Process Control 24 (5) (2014) 663–671, http://dx.doi.org/10.1016/j.jprocont.2014.03.011.
[20] L. Fu, Ü. Özgüner, Extremum seeking with sliding mode gradient estimation and asymptotic regulation for a class of nonlinear systems, Automatica 47 (12) (2011) 2595–2603, http://dx.doi.org/10.1016/j.automatica.2011.09.031.
[21] H. De Battista, J. Picó, F. Garelli, A. Vignoni, Specific growth rate estimation in (fed-)batch bioreactors using second-order sliding observers, J. Process Control 21 (7) (2011) 1049–1055, http://dx.doi.org/10.1016/j.jprocont.2011.05.008.
[22] S. Nuñez, H. De Battista, F. Garelli, A. Vignoni, J. Picó, Second-order sliding mode observer for multiple kinetic rates estimation in bioprocesses, Control Eng. Pract. 21 (9) (2013) 1259–1265.
[23] R. Fletcher, Practical Methods of Optimization, Wiley, Chichester, New York, 1987.
[24] A. Levant, Robust exact differentiation via sliding mode technique, Automatica 34 (3) (1998) 379–384.
[25] J. Moreno, E. Guzmán, Super-twisting observer for second-order systems with time-varying coefficient, IET Control Theory Appl. 9 (4) (2015) 553–562, http://dx.doi.org/10.1049/iet-cta.2014.0348.
[26] J. Picó, H. De Battista, F. Garelli, Smooth sliding-mode observers for specific growth rate and substrate from biomass measurement, J. Process Control 19 (8) (2009) 1314–1323.
[27] J. Cortes, Discontinuous dynamical systems, IEEE Control Syst. 28 (3) (2008).
[28] A.F. Filippov, Differential Equations with Discontinuous Righthand Sides, vol. 18, Springer Science & Business Media, 2013.
[29] J.A. Moreno, M. Osorio, Strict Lyapunov functions for the super-twisting algorithm, IEEE Trans. Autom. Control 57 (4) (2012) 1035–1040.
[30] H.K. Khalil, Noninear Systems, Prentice-Hall, New Jersey, 1996.
[31] V.I. Zubov, L.F. Boron, Methods of AM Lyapunov and Their Application, Noordhoff Groningen, 1964.
[32] A. Poznyak, Advanced Mathematical Tools for Automatic Control Engineers, Elsevier, Amsterdam Boston, 2008.
[33] A. Bacciotti, L. Rosier, Lyapunov Functions and Stability in Control Theory, Springer Science & Business Media, 2006.
[34] V.I. Bogachev, Measure Theory, vol. 1, Springer Science & Business Media, 2007.
[35] A. Isidori, Nonlinear Control Systems II, Springer-Verlag London, 1999.
[36] J. Moreno, Lyapunov approach for analysis and design of second order sliding mode algorithms, in: L. Fridman, J. Moreno, R. Iriarte (Eds.), Sliding Modes After the First Decade of the 21st Century, Lecture Notes in Control and Information Sciences, vol. 412, Springer Berlin Heidelberg, 2012, pp. 113–149, http://dx.doi.org/10.1007/978-3-642-22164-4 4.
[37] M.S.I. Mozumder, L. Goormachtigh, L. Garcia-Gonzalez, H. De Wever, E.I.P. Volcke, Modeling pure culture heterotrophic production of polyhydroxybutyrate (PHB), Bioresour. Technol. 155 (2014) 272–280.
[38] M. Jamilis, F. Garelli, M.S.I. Mozumder, E. Volcke, H. De Battista, Specific growth rate observer for the growing phase of a polyhydroxybutyrate production process, Bioprocess Biosyst. Eng. 38 (3) (2015) 557–567.